A METHOD FOR FLUID-STRUCTURE INTERACTION PROBLEMS WITH NON-NEWTONIAN FLUID

A. Amani, A. Naseri, C. D. Pérez-Segarra and A. Oliva

Heat and Mass Transfer Technological Center (CTTC)
Universitat Politécnica de Catalunya - BarcelonaTech (UPC)
ESEIAAT, C/ Colom 11, 08222 Terrassa (Barcelona), Spain
e-mail: anaseri@cttc.upc.edu, web page: http://www.cttc.upc.edu/

Key words: Fluid-Structure Interaction, non-Newtonian Fluid

Abstract. This paper represents a numerical method to solve fluid-structure interaction (FSI) problems where the fluid exhibits a non-Newtonian Viscoelastic behaviour. Oldroyd-B constitutive equation is used to model Viscoelastic fluid. For FSI solution, a semi-implicit partitioned method is used which separates the fluid pressure term and strongly couples it to the structure, while the remaining fluid terms are only weakly coupled. Numerical tests demonstrate the capability of the method to solve FSI problems with a non-Newtonian Viscoelastic behaviour of the fluid.

1 INTRODUCTION

Fluid-structure interaction (FSI) problems include a fluid flow mutually interacting with a moving or deforming structure. Fluid flow exerts surface forces on the solid wet boundary and the movement of the structure alters the fluid motion. There is a wide range of applications cited for FSI, from civil to biomedical engineering. Many numerical methods have been developed to accurately simulate FSI problems. However, most of the previous works have studied the interaction of a Newtonian fluid with an elastic structure. Although Newtonian fluids account for many important problems, there are many practical situations where the working fluid cannot be modeled as Newtonian. Thus the mathematical model for simulation of the FSI problem must account for the non-Newtonian behavior of the fluid as well. Despite many numerical methods have been proposed for non-Newtonian fluids, few works in the literature have studied the problem of a non-Newtonian fluid interacting with a deforming structure.

Partitioned methods are a favorable class of numerical techniques to solve FSI problems (see [1] for a review). A separate solver is used for each sub-problem domain and the equilibrium between the domains is enforced as coupling condition on the interface. Partitioned methods could be weakly-coupled (explicit) or strongly-coupled (implicit) depending on how the equilibrium condition is enforced. Weakly-coupled methods do not observe the equilibrium condition exactly which might cause numerical instability in FSI

problems with low solid/fluid density ratios (so-called added-mass effect) [2, 3]. Strongly-coupled methods enforce the equilibrium condition via coupling iterations between the fluid and structural solvers. These methods are stable for FSI problems with strong added-mass effect, although they are computationally expensive due to the coupling iterations. A third technique, called semi-implicit method, segregates the fluid pressure term and strongly couples it to the structure. Strong coupling of the fluid pressure guarantees the stability of the method while weak coupling of the remaining terms reduces the computational effort [4, 5].

Viscoelastic behaviour of fluid is prevalent in a wide range of applications including food processing, pharmaceuticals, casting industry and chemical industry [6]. One of the important applications of Viscoelastic fluids is in microfluidic devices, for instance memory and control devices [7] and microfluidic rectifiers [8], use Viscoelastic materials as working fluid. A huge portion of biological fluids in nature exhibit viscoelastic behavior. Thus it is important to understand the dynamics of Viscoelastic fluids. Numerical simulation has become a powerful method in studying the underlying physics of viscoelastic behaviour of the fluid and also an important tool in design and manufacturing process of Viscoelastic applications. In numerical simulations, the Viscoelastic flow is solved using Navier-Stokes equations integrated with an extra constitutive equations which describes the relation of stress with strain rate tensor [9]. A variety of numerical methods, including finite difference, finite element, finite volume and hybrid methods, have been developed to simulate viscoelastic flows [10, 11, 12, 13]. In spite of significant progress in the field of single phase viscoelastic fluid flow, the key questions in the field of non-Newtonian Viscoelastic Fluid-Structure Interaction (nVFSI) has not been answered. In this paper we propose a numerical method to study the non-Newtonian Viscoelastic fluid interacting with an elastic structure. Oldroyd-B constitutive equation is used to model the viscoelastic fluid.

The rest of the paper is organized follows: Governing equations are presented in section 2. Numerical methods are presented in section 3. The results are discussed in section 4 and finally the conclusion remarks are presented in section 5.

2 GOVERNING EQUATIONS

In this section, the governing equations for each sub-problem domain and the coupling conditions on the interface are presented. The fluid and structural domains are referred to as $\Omega_f(t)$ and $\Omega_s(t)$ respectively, as they both vary in time. The interface of the domains is the shared boundary denoted by $\Gamma(t) = \partial\Omega_f(t) \cap \partial\Omega_s(t)$.

2.1 Fluid equations

The unsteady flow of an incompressible fluid is governed by the Navier-Stokes equations. An Arbitrary Lagrangian-Eulerian (ALE) formulation of these equations in a moving domain is given by:

$$\frac{\partial \mathbf{u}}{\partial t} + \mathbf{c} \cdot \nabla \mathbf{u} = \frac{1}{\rho_f} \nabla \cdot \boldsymbol{\sigma}_f \tag{1}$$

$$\nabla \cdot \mathbf{u} = 0 \tag{2}$$

where $\mathbf{u}$ is the fluid velocity and ρ_f the fluid density. Vector $\mathbf{c}$ is the ALE convective velocity $\mathbf{c} = \mathbf{u} - \mathbf{w}$, which is the fluid velocity relative to a domain moving with a velocity $\mathbf{w}$. The stress tensor $\boldsymbol{\sigma}_f$ is defined as:

$$\boldsymbol{\sigma}_f = -p\mathbf{I} + 2\mu_s\boldsymbol{\gamma} + \mu_p\boldsymbol{\tau} \tag{3}$$

where p is the fluid pressure, $\mathbf{I}$ the unit tensor, μ_s the dynamic viscosity of the solvent fluid, μ_p is the dynamic viscosity of the polymer fluid and $\boldsymbol{\gamma}$ the strain rate tensor given by:

$$\boldsymbol{\gamma} = \frac{1}{2}(\nabla\mathbf{u} + \nabla\mathbf{u}^T) \tag{4}$$

In euqation 3, $\boldsymbol{\tau}$ is the extra stress tensor related to non-Newtonian viscoelastic behaviour of the fluid. The Oldroyd-B constitutive equation is used to model this extra stress tensor as follow:

$$\boldsymbol{\tau} + \lambda_1\overset{\nabla}{\boldsymbol{\tau}} = 2\mu_0(\boldsymbol{\gamma} + \lambda_2\overset{\nabla}{\boldsymbol{\gamma}}) \tag{5}$$

where μ_0 is the total viscosity of the fluid ($\mu_0 = \mu_s + \mu_p$), λ_1 is the relaxation time and λ_2 is the retardation time ($\lambda_2 = \mu_s/\mu_0\lambda_1$). In this formulation $\overset{\nabla}{\boldsymbol{\tau}}$ and $\overset{\nabla}{\boldsymbol{\gamma}}$ are the upper convected time derivative of stress and strain rate tensors, respectively. This operator for an arbitrary tensor of $\boldsymbol{A}$ defines as:

$$\overset{\nabla}{\boldsymbol{A}} = \frac{\partial \boldsymbol{A}}{\partial t} + \boldsymbol{u}.\nabla\boldsymbol{A} - \nabla\boldsymbol{u}^T.\boldsymbol{A} - \boldsymbol{A}.\nabla\boldsymbol{u} \tag{6}$$

2.2 Structural equations

The structural domain is governed by the nonlinear elastodynamics equation:

$$\rho_s\frac{D^2\mathbf{d}}{Dt^2} = \nabla \cdot \boldsymbol{\sigma}_s \tag{7}$$

where $\mathbf{d}$ stands for the structural position with respect to the reference configuration, and the structural density is shown by ρ_s. The Cauchy stress tensor $\boldsymbol{\sigma}_s$ is related to the second Piola-Kirchhoff tensor $\mathbf{S}_s$ by:

$$\mathbf{S}_s = J\mathbf{F}^{-1}\boldsymbol{\sigma}_s\mathbf{F}^T \tag{8}$$

where $\mathbf{F}$ is the deformation gradient $\mathbf{F} = \nabla\mathbf{d}$ and J is its determinant ($J = det(\mathbf{F})$).

The FSI method is presented for a general structure, however, for the test case in this paper the structure is considered to be an Euler-Bernoulli beam, governed by the following equation:

$$\rho_sA\frac{\partial^2\mathbf{d}}{\partial t^2} + EI\frac{\partial^4\mathbf{d}}{\partial x^4} = q(x,t) \tag{9}$$

3

where $\mathbf{d} = [0, y, 0]^T$ in a Cartesian coordinate (x, y, z), A is the cross section area of the beam, I the second moment of area, and q is the normal load per unit length.

2.3 Coupling conditions

The coupling conditions apply at the interface Γ and account for the interaction of the domains. They are derived from the kinematic and dynamic equilibrium between the domains, which yield to the following conditions on a non-slip type interface:

$$\mathbf{u}_\Gamma = \frac{\partial \mathbf{d}_\Gamma}{\partial t} \tag{10}$$

$$\boldsymbol{\sigma}_s \cdot \mathbf{n}_\Gamma = \boldsymbol{\sigma}_f \cdot \mathbf{n}_\Gamma \tag{11}$$

for any point $\mathbf{x} \in \Gamma$, where $\mathbf{n}_\Gamma$ is the unit normal vector on the interface. Equation (10) represents equality of the velocity of the fluid and the structure on the interface to assure the kinematic equilibrium. Equation (11) represents equality of the traction on the interface for dynamic equilibrium.

3 NUMERICAL METHOD

In this section we represent the numerical methods and discretization schemes to solve the coupled non-linear system of governing equations.

3.1 Fluid solver

A fractional-step (projection) method [14] is used to solve the velocity/pressure coupling of the momentum equation. Thus, an intermediate velocity field is evaluated without considering the pressure gradient term. We use an explicit Adams-Bashforth method for discretization of the convective and diffusive terms. Therefore the intermediate velocity field is evaluated as:

$$\frac{\mathbf{u}^* - \mathbf{u}^n}{\Delta t} = \frac{3}{2}[-(\mathbf{c} \cdot \nabla \mathbf{u})^n + \frac{\mu_s}{\rho_f}\nabla^2 \mathbf{u}^n + \mu_p \nabla . \boldsymbol{\tau}^n] - \frac{1}{2}[-(\mathbf{c} \cdot \nabla \mathbf{u})^{n-1} + \frac{\mu_s}{\rho_f}\nabla^2 \mathbf{u}^{n-1} + \mu_p \nabla . \boldsymbol{\tau}^{n-1}] \tag{12}$$

for any $\mathbf{x} \in \Omega_f^{n+1}$. This velocity field is then projected onto a space of divergence-free vector fields:

$$\mathbf{u}^* = \mathbf{u}^{n+1} + \frac{\Delta t}{\rho_f}\nabla p^{n+1} \tag{13}$$

$$\nabla \cdot \mathbf{u}^{n+1} = 0 \tag{14}$$

where p^{n+1} is the pressure field obtained by:

$$\nabla^2 p^{n+1} = \frac{\rho_f}{\Delta t}\nabla \cdot \mathbf{u}^* \tag{15}$$

The boundary condition for velocity on the interface comes from the coupling condition:

$$\mathbf{u}_\Gamma^{n+1} = \frac{\mathbf{d}_\Gamma^{n+1} - \mathbf{d}_\Gamma^n}{\Delta t} \tag{16}$$

for any $\mathbf{x} \in \Gamma^{n+1}$. We apply this boundary condition on the predicted velocity as well:

$$\mathbf{u}_\Gamma^* = \frac{\mathbf{d}_\Gamma^{n+1} - \mathbf{d}_\Gamma^n}{\Delta t} \tag{17}$$

In this work, the fractional-step method is used not only for solving the fluid equations, but also as a framework for the overall FSI solution algorithm, making it fundamental to the overall method.

3.2 Dynamic mesh

As the solid boundary is deformable, fluid mesh needs to move to adapt to the new location of the interface and the discrete domain velocity on the mesh surfaces $\mathbf{w}^{n+1}$ needs to be evaluated. A parallel moving mesh technique, based on radial basis function interpolation method [15], is used to move the fluid grid in accordance to the new location of the interface. Surface velocities are evaluated according to the so-called space conservation law which guarantees no volume is lost while moving the grid. Detailed description of the dynamic mesh method could be found in [15, 5]. Here we will use the function $\mathcal{M}$ to refer to the mesh movement step:

$$(\Omega_f^{n+1}, \mathbf{w}^{n+1}) = \mathcal{M}(\mathbf{d}_\Gamma^{n+1}) \tag{18}$$

3.3 Structural solver

Structural equations are discretized in time using a second-order Newmark method. Defining the structural velocity $\mathbf{v} = \frac{\partial \mathbf{d}}{\partial t}$, the semi-discretized structural equation reads:

$$\mathbf{v}^{n+1} = \mathbf{v}^n + \frac{\Delta t}{2\rho_s A}[(q^{n+1} - EI\frac{\partial^4 \mathbf{d}}{\partial x^4})^{n+1} + (q^n - EI\frac{\partial^4 \mathbf{d}}{\partial x^4})^n] \tag{19}$$

and the new location of the structure could be calculated as:

$$\mathbf{d}^{n+1} = \mathbf{d}^n + \frac{\Delta t}{2}(\mathbf{v}^{n+1} + \mathbf{v}^n) \tag{20}$$

It should be noted that using a simplified structural model is not restrictive for the proposed FSI coupling method, since it is used as a black-box module. We will use the notation $\mathcal{S}$ to refer to the structural solver as a function of surface stress on the interface:

$$\mathbf{d}_\Gamma = \mathcal{S}(\boldsymbol{\sigma}_\Gamma) \tag{21}$$

where $\mathbf{d}_\Gamma$ is the location of the interface and $\boldsymbol{\sigma}_\Gamma$ is the stress on the interface exerted by the fluid $\boldsymbol{\sigma}_\Gamma = \boldsymbol{\sigma}_f(p, \mathbf{u})_\Gamma \cdot \mathbf{n}_\Gamma$.
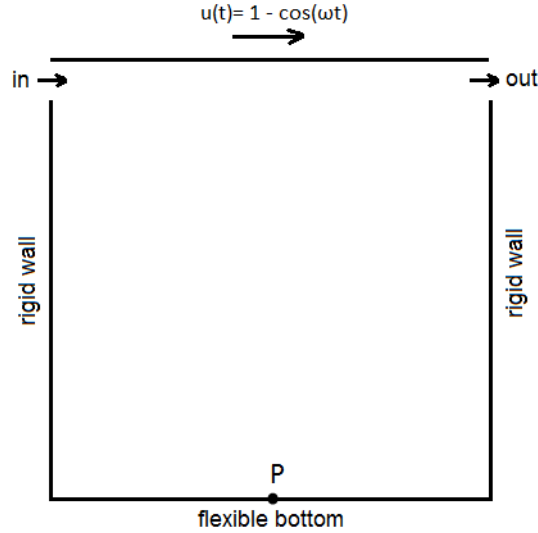
Figure 1: Schematic view of the driven cavity test case with flexible bottom wall. Point P is the midpoint of bottom wall.

3.4 Coupling method

A semi-implicit FSI coupling method is used in which only the fluid pressure term is strongly coupled to the structure via coupling iterations. The remaining fluid terms as well as the dynamic mesh step are evaluated only once per time step [16, 5].

The FSI solution method at a new time step is as follows.

step 1- Explicit step:

- Predict the location of the interface by extrapolation from previous time steps.

- Define the new discretized domain using equation 18.

- Evaluate the predicted velocity field by equation 12.

step 2- Implicit step:

- Evaluate the fluid pressure (equation 15)

- Solve the structural equations to evaluate the deformation (equation 21).

- Update the boundary condition on predicted velocity (equation 17).

- Repeat until convergence is achieved.

step 3- Explicit step:

- Correct the velocity field (equation 13)

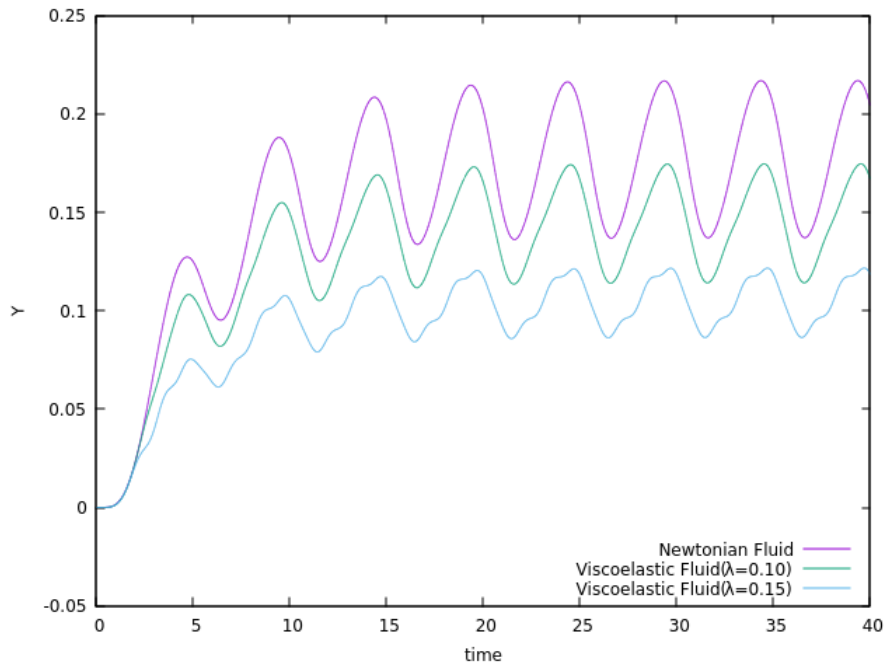- Apply the boundary condition for velocity (equation 16).

6

Figure 2: Oscillation in the position of the point P for three different cases of Newtonian fluid, and Viscoelastic fluids with $\lambda_1 = 0.10$ and $\lambda_1 = 0.15$

Step 2 of the above algorithm is where fluid pressure is strongly coupled to the structure. This step provides for the stability of the method for FSI problems with strong added-mass effect. The FSI coupling method is extensively tested and validated in the previous works of the authors [16, 5, 17, 18].

4   NUMERICAL TESTS

Numerical tests are carried out on a benchmark problem studied in [3, 19], among others. The test case is a 2-D lid-driven cavity of a $1m \times 1m$ with a flexible bottom. The top boundary of the cavity is moving with an oscillatory speed of $u(t) = 1 - cos(\omega t)$ with $\omega = 2\pi/5$. There are two openings of $0.1m$ length on the sidewalls that allow the fluid to enter to and exit from the domain. Figure 1 shows a schematic description of the problem.

The fluid density in all the cases is $\rho_f = 1.0kg/m^3$. For Newtonian fluid, viscosity is $\mu_s = 0.01$ Pa.s and for viscoelastic fluids, $\mu_s = \mu_p = 0.005$ Pa.s. Two different viscoelastic cases with λ_1 values of 0.1 and 0.15 are tested and results are compared with the results of Newtonian fluid. The flexible structure at the bottom has a thickness of $h = 0.05m$, the structural density is $\rho_s = 20kg/m^3$ and the Young modulus $E = 250N/m^2$.

The flexible bottom is modeled as an Euler-Bernoulli beam, as mentioned earlier. A 51×51 spatial grid is used to solve the problem. Spatial discretization is carried out using a finite volume method with second-order central difference schemes. The structure is a thin membrane so the fluid mesh elements on the interface are also used as the computational grid for the structural equations. Thus, the structural grid nodes match the fluid mesh on
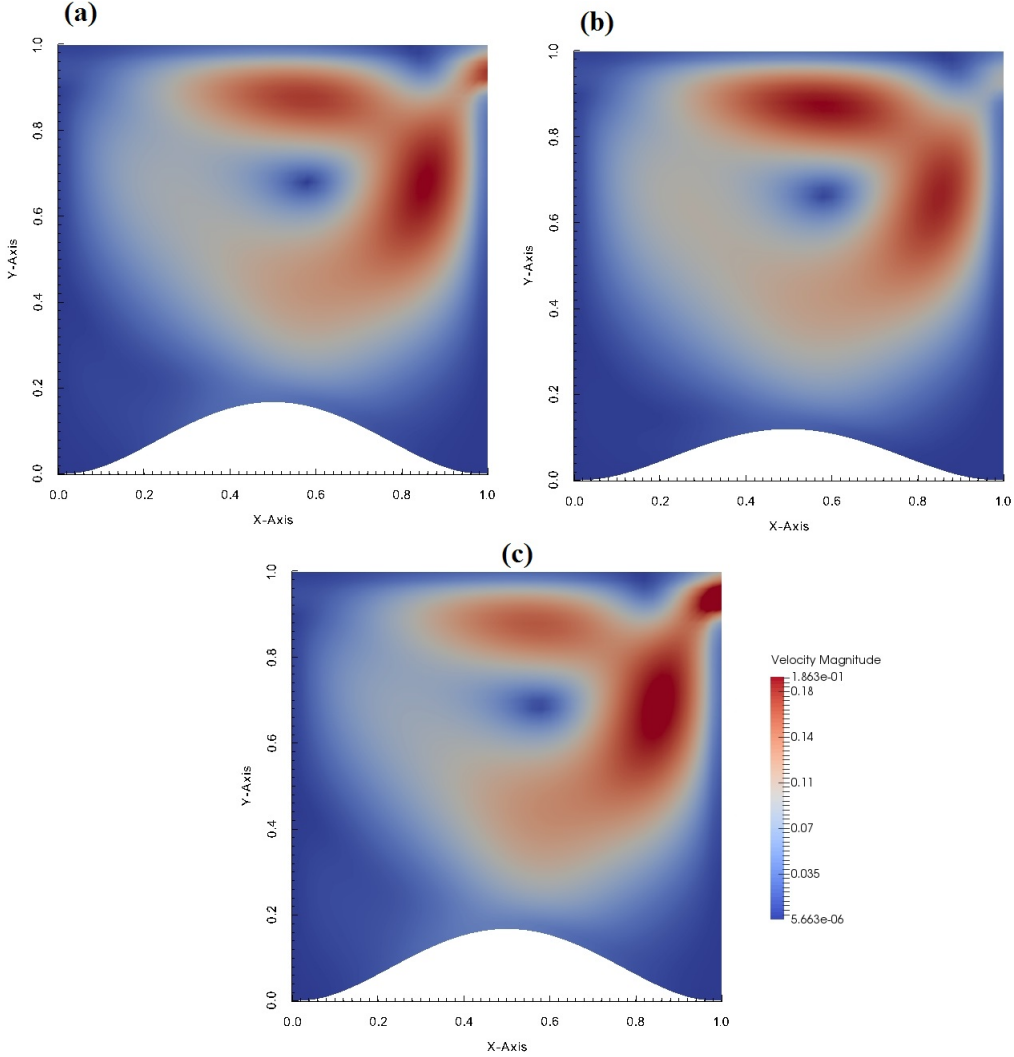
Figure 3: Velocity Magnitude field inside of the deformed domain at time $t = 40s$. (a): Viscoelastic fluid with $\lambda_1 = 0.1$, (b): viscoelastic fluid with $\lambda_1 = 0.15$ and (c): Newtonian fluid.

the interface and there is no need for interpolation of parameters between the domains. Simulations are carried out from $t = 0$ until $t = 40s$. Figure 2 presents the oscillation in the position of the point P for three different cases of Newtonian fluid, and Viscoelastic fluids with $\lambda_1 = 0.10$ and $\lambda_1 = 0.15$.

It is plain to see that by varying from Newtonian fluid to Viscoelastic fluid with $\lambda_1 = 0.10$, the magnitude of the structural deformation has decreased noticeably. Moreover, by increasing the relaxation time of the Viscoelastic fluid from 0.10 to 0.15, the nature of the movement of the point P changes from smooth oscillation to a rough shape. Figure 3 shows the flow field inside the domain with structural deformation at the bottom for the aforementioned cases, at $t = 40s$. It can be seen in this figure that the oscillation magnitude of Newtonian fluid is bigger than the others as well as the velocity magnitude at the outlet.

5 CONCLUSIONS

A Numerical method for simulations of non-Newtonian Viscoelastic fluid-structure interaction (nVFSI) is presented. Oldroyd-B model is used as the constitutive equation for Viscoelastic fluid and a semi-implicit partitioned method is used for FSI coupling. Three different cases of Newtonian fluid and Viscoelastics with $\lambda_1 = 0.10$ and $\lambda_1 = 0.15$ are tested. The results show that by including the Viscoelastic behaviour to the system, the magnitude of the deformation of the structure decreases. Also by increasing the relaxation time from 0.10 to 0.15, the nature of the deformation of the bottom wall changes from smooth to non-smooth oscillation.

6 Acknowledgement

REFERENCES

[1] Joris Degroote. *Arch. Comput. Methods Eng.*, 20:185–238, 2013.

[2] P. Causin, J. F. Gerbeau, and F. Nobile. *Comput. Methods Appl. Mech. Eng.*, 194:4506–4527, 2005.

[3] C. Förster, W. A. Wall, and E. Ramm. *Comput. Methods Appl. Mech. Eng.*, 196:1278–1293, 2007.

[4] M. A. Fernández, J-F Gerbeau, and C. Grandmont. *Int. J. for Numer. Methods Eng.*, 69(4):794–821, 2007.

[5] A. Naseri, O. Lehmkuhl, I. Gonzalez, E. Bartrons, C. D. Pérez-Segarra, and A. Oliva. *J. Fluids Struct.*, 80:94–112, 2018.

[6] Todd M. Squires and Stephen R. Quake. *Rev. Mod. Phys.*, 77:977–1026, Oct 2005.

[7] Alex Groisman, Markus Enzelberger, and Stephen R. Quake. *Sci.*, 300(5621):955–958, 2003.

[8] Alex Groisman and Stephen R. Quake. *Phys. Rev. Lett.*, 92:094501, Mar 2004.

[9] Alexander N. Morozov and Wim van Saarloos. *Phys. Reports*, 447(3):112 – 143, 2007. Nonequilibrium physics: From complex fluids to biological systems I. Instabilities and pattern formation.

[10] M.J. Crochet and G. Pilate. *J. Non-Newtonian Fluid Mech.*, 1(3):247 – 258, 1976.

[11] Robert E. Gaidos and Ron Darby. *J. Non-Newtonian Fluid Mech.*, 29:59 – 79, 1988.

[12] S.S Edussuriya, A.J Williams, and C Bailey. *J. Non-Newtonian Fluid Mech.*, 117(1):47 – 61, 2004.

[13] J.E. Lpez-Aguilar, M.F. Webster, H.R. Tamaddon-Jahromi, and O. Manero. *J. Non-Newtonian Fluid Mech.*, 222:190 – 208, 2015. Rheometry (and General Rheology): Festschrift dedicated to Professor K Walters FRS on the occasion of his 80th birthday.

[14] A. J. Chorin. *Math. Comput.*, 22:745–762, 1968.

[15] O. Estruch, O. Lehmkuhl, R. Borrell, C. D Pérez Segarra, and A. Oliva. *Comput. Fluids*, 80:44–54, 2013.

[16] A. Naseri, O. Lehmkuhl, I. Gonzalez, and A. Oliva. *J. Phys. Conf. Ser.*, 745(3):032020, 2016.

[17] I González, O Lehmkuhl, A Naseri, J Rigola, and A Oliva. In *International Compressor Engineering Conference*, page 2490. Purdue University Libraries, 2016.

[18] I. González, A. Naseri, J. Rigola, C. D. Pérez-Segarra, and A. Oliva. *IOP Conf. Ser. Mater. Sci. Eng*, 232(1):012032, 2017.

[19] U. Küttler and W. A. Wall. *Comput. Mech.*, 43:61–72, 2008.